ORIGINAL PAPER

Effects of seawater pCO$_2$ on the skeletal morphology of massive *Porites* spp. corals

Nicola Allison[1] · Phoebe Ross[1,5] · Alex Brasier[2] · Nadia Cieminska[1] · Nicolas Lopez Martin[1] · Catherine Cole[1,6] · Chris Hintz[3] · Ken Hintz[4] · Adrian Finch[1]

Abstract

Ocean acidification alters the dissolved inorganic carbon chemistry of seawater and can reduce the calcification rates of tropical corals. Here we explore the effect of altering seawater pCO$_2$ on the skeletal morphology of 4 genotypes of massive *Porites* spp. which display widely different calcification rates. Increasing seawater pCO$_2$ causes significant changes in in the skeletal morphology of all *Porites* spp. studied regardless of whether or not calcification was significantly affected by seawater pCO$_2$. Both the median calyx size and the proportion of skeletal surface occupied by the calices decreased significantly at 750 µatm compared to 400 µatm indicating that polyp size shrinks in this genus in response to ocean acidification. The coenosteum, connecting calices, expands to occupy a larger proportion of the coral surface to compensate for this decrease in calyx area. At high seawater pCO$_2$ the spines deposited at the skeletal surface became more numerous and the trabeculae (vertical skeletal pillars) became significantly thinner in 2 of the 4 genotypes. The effect of high seawater pCO$_2$ is most pronounced in the fastest growing coral and the regular placement of trabeculae and synapticulae is disturbed in this genotype resulting in a skeleton that is more randomly organised. The study demonstrates that ocean acidification decreases the polyp size and fundamentally alters the architecture of the skeleton in this major reef building species from the Indo-Pacific Ocean.

Keywords Coral · Calcification · Skeleton · Polyp size · Ocean acidification

Introduction

Tropical corals produce the skeletons that underpin coral reef structures and provide habitat spaces for a diverse range of biota. In 2015 the value of tropical coral reefs as resources for fisheries, tourism and land protection was estimated to exceed US$30 billion annually (Chen 2015). Increasing atmospheric CO$_2$ is altering the chemistry of seawater, decreasing ocean pH (IPCC 2019) and reducing the calcification of many tropical corals (Erez et al. 2011). Corals build the skeleton at calcification sites which are isolated from seawater either from media contained between the coral tissue and the skeleton (Allemand et al. 2011) or in intracellular vesicles (Drake et al. 2018). The coral increases the pH of the calcification media above that of seawater (Al Horani et al. 2003; Venn et. al. 2011). This shifts the dissolved inorganic carbon equilibrium to increase CO$_3^{2-}$, one of the substrates for CaCO$_3$ formation, and likely promotes calcification. However, in corals cultured under high seawater pCO$_2$, the pH of the calcification media is lower than in corals cultured at lower pCO$_2$ (Venn et al. 2013; Allison

✉ Nicola Allison
na9@st-andrews.ac.uk

1   School of Earth and Environmental Sciences, University of St. Andrews, St. Andrews KY16 9TS, UK

2   School of Geosciences, University of Aberdeen, Meston Building, Aberdeen AB24 3UE, UK

3   Department of Marine and Environmental Sciences, Savannah State University, Savannah, GA, USA

4   Department of Electrical and Computer Engineering, George Mason University, Fairfax, VA, USA

5   Present Address: Department of Earth Science and Engineering, Imperial College London, London, UK

6   Present Address: Graduate School of the Environment, Centre for Alternative Technology, Powys SY20 9AZ, UK

et al. 2021) and this likely decreases the proportion of DIC present as $[CO_3^{2-}]$.

Coral skeletons are organic:inorganic composites composed of the mineral aragonite and biomolecules, e.g., proteins and polysaccharides, secreted by the coral (Falini et al. 2015). The concentration of the skeletal organic matrix and its constituents has been observed to increase in response to rising seawater pCO_2 (Tambutte et al. 2015, Coronado et al. 2019, Kellock et al. 2020). $CaCO_3$ precipitation can be promoted and inhibited by biomolecules (Elhadj et al. 2006) and the organic matrix extracted from biogenic calcareous structures can influence both the morphology of $CaCO_3$ crystals precipitated in vitro (Falini et al. 2013) and their physical properties (Herman et al. 1988; Kim et al. 2016). Alterations in the concentration or composition of the skeletal organic matrix may account for the changes in coral skeletal architecture which can be observed in response to high seawater pCO_2 e.g., increases in calyx size (Tambutte et al. 2015), variations in crystal appearance (Coronado et al. 2019) and decreases in the abundance of the rapid accretion deposits on the skeletal surface (Scucchia et al. 2021).

In this study we investigated the effect of changes in seawater pCO_2 on the skeletal morphology of cultured massive *Porites* spp. Massive *Porites* spp. can be important contributors to reef building in the Indo-Pacific (Veron 1993) and may be relatively resilient to rising seawater pCO_2. *Porites* spp. persist at naturally high pCO_2 reef sites (Fabricius et al. 2011; Crook et al. 2012) and may even increase their coverage compared to adjacent lower pCO_2 control sites (Fabricius et al. 2011). The calcification, photosynthesis and respiration rates of the corals examined in the current study were reported by Cole et al. 2018. Increasing seawater pCO_2 decreased calcification significantly in some *Porites* spp. individuals but not in others (Cole et al. 2018). This contrasts with a study of juvenile Porites which found no significant effect of seawater pCO_2 on calcification (Edmunds 2012). For the present study we compare the sizes of key skeletal features (calyx size and trabecula width) between seawater pCO_2 treatments and explore the skeletal morphology by scanning electron microscopy. We examine 2 *Porites* species (*P. lutea* and *P. murrayensis*) and include different individuals which either exhibited reduced calcification rates at high seawater pCO_2 or appeared unaffected (Cole et al. 2018).

Materials and methods

Coral culturing

We cultured massive *Porites* spp. corals over a range of seawater pCO_2 (~ 180, 400 and 750 µatm) in two experiments, previously described (Cole et al. 2016, 2018). Full details

of the methodology and seawater chemistry are provided in Appendix A. These pCO_2 reflect conditions in the Last Glacial Maximum, the present day and a potential future CO_2 scenario (Barry et al. 2011). In the first experiment corals were maintained at target pCO_2 and 25 °C for 6–7 months before sacrifice. In the second experiment corals were maintained at target pCO_2 and 28 °C for 5–6 months before the temperature was decreased to 25 °C over a period of 1 month and then the corals held at this temperature for 9 weeks before sacrifice. For each experiment we sawed imported coral heads into multiple pieces (each ~ 12 cm in diameter) so that at least one large piece of each head could be cultured in each seawater pCO_2 treatment. The corals were considered to represent different genotypes when they were collected from spatially separate (non-adjoining) colonies. Although the temperature regimes vary between the two experiments we compare variations in skeletal morphology within each coral genotype. All coral skeletons were cleaned with sodium hypochlorite and rinsed and dried before analysis. We examined the skeletal morphology of 4 genotypes (numbered 1, 4, 6 and 7, following the convention used in Cole et al. 2018). Genotypes 1 and 7 were identified as *P. lutea* and genotypes 4 and 6 were identified as *P. murrayensis* on the basis of corallite structure (Veron 1993). In 2 genotypes (4 and 7) calcification was significantly reduced at 750 µatm pCO_2 compared to 180 µatm, while in the other 2 genotypes (1 and 6), calcification rate differences were not significant (Cole et al. 2018).

Samples with a surface area of 1–3 cm² were cut from the surface of each skeleton using a handheld circular saw, cleaned in an ultrasonic bath and dried before imaging of the skeletal surface. Cross section samples through the coral skeleton were prepared by cutting a slice through the centre of the coral heads and then cutting a strip of skeleton about 10 mm wide along the maximum growth axis of the slice. The outermost 1.5 cm on the strips were fixed in 25 mm circular epoxy resin blocks (Epofix, Struers Ltd.), polished with silicon carbide papers and alumina (Allison et al. 2021) and photographed under reflected light microscopy.

Corallite measurements

The skeleton surfaces were photographed using a Keyence VHX-2000E digital microscope. The focus-stacking function was used to create in-focus images of the three dimensional surface with each image recording an area of 5.2 × 6.9 mm. We recorded 4 or more images of each coral skeleton, focusing on areas at the centre of each skeleton, where growth rate was maximal and avoiding depressions, where corallites were growing towards each other.

The key skeletal structures examined in this study are illustrated in Fig. 1. *Porites* spp. corals are colonial and composed of multiple polyps. The skeleton deposited by
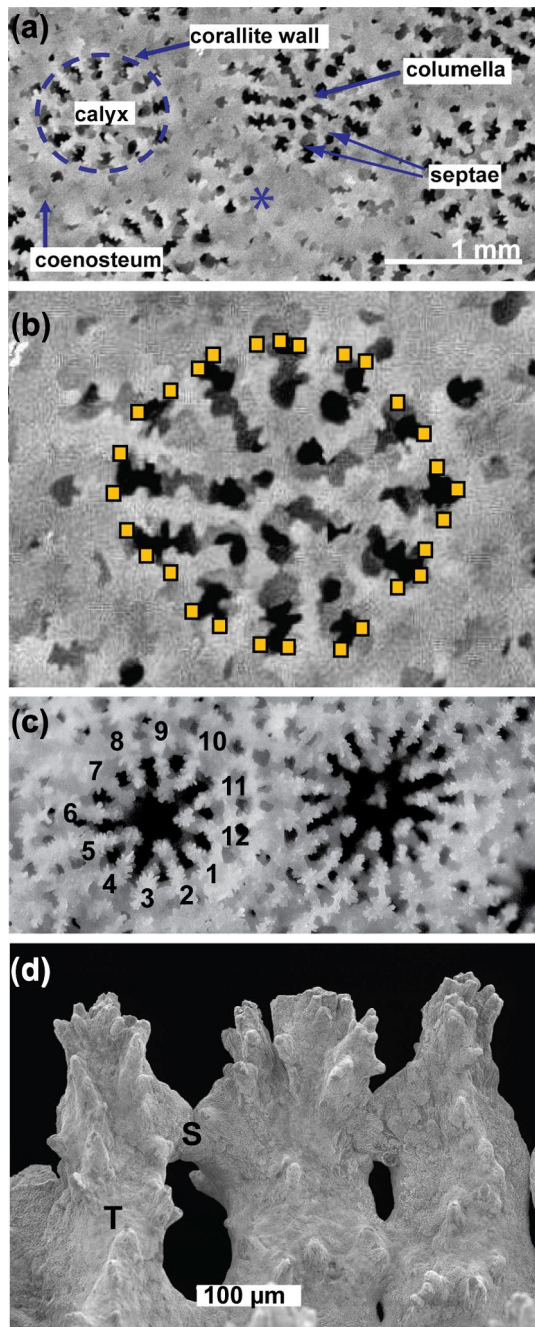
Fig. 1 Photomicrographs of **a** a *P. lutea* skeleton with key skeletal structures annotated, * marks a new polyp forming by extratentacular budding, **b** positions of line segments in ImageJ to estimate calyx area in a typical corallite and **c** surface of a *P. murrayensis* specimen. Twelve septae are typically visible in each corallite (see numbers on left hand polyp) but in some relatively large corallites more septae are visible (right hand polyp) suggestive of polyp division by intratentacular budding. **d** Skeletal trabeculae (T) and synapticulae (S) at the very surface of the skeleton

each polyp is called a corallite (Fig. 1a). At the centre of each corallite is a calyx (plural calices), an approximately circular cup that houses the polyp. Vertical partitions called septae radiate from the corallite wall towards the

centre of the calyx. At the centre of the corallite, extensions of the septae may intertwine to form a columella, a structure present in some *Porites* species, e.g., *P. lutea* but absent in others, e.g., *P. murrayensis*. Individual calices are joined by the coenosteum, the skeleton deposited between polyps. In this study we determined the surface area of the coral calices at the surface of the skeleton and calculated the % of surface area that was occupied by polyps (in contrast to coenosteum).

The area of each calyx in each image was measured on scaled photographs using the image processing software, ImageJ (National Institute of Health, USA). Using the polygon selection tool we create line segments along the internal edge of the corallite wall and at the intersection of septa and the corallite wall (Fig. 1b). The software interpolated between these segments and calculated the calyx surface area. We combined the measurements of all whole calices, i.e., where the photograph recorded the whole calyx and did not cut off part of the structure, to determine the size distribution of polyps in the coral. For each image the area of all calices in the image (both whole and partial corallites) was summed and divided by the total surface area of the image to each provide an estimate of the percentage of the skeletal surface occupied by polyps (compared to the coenosarc tissue interconnecting the polyps). We explored the impact of seawater pCO_2 on calyx sizes and calyx:coenosteum ratio in the different coral genotypes. The entire skeleton is composed of vertical pillars, called trabeculae, which are interconnected by horizontal rungs, called synapticulae (Fig. 1d). We used the cross section photographs to measure the widths of the trabeculae in each coral at a depth of 1 mm from the coral surface. Calcification rates varied from 4 to 35 µmol cm^{-2} day^{-1} at 25 °C in the corals examined here (Cole et al. 2018) so this position in the skeleton represents a different timepoint in each coral. We measured trabecula widths at this position to ensure we compared comparable spatial positions in the skeleton.

Scanning electron microscopy

Scanning electron micrograph images were collected for genotypes 4, 6 and 7. Skeletal samples were mounted on aluminium pin stubs (25 mm diameter) using double-sided carbon adhesive discs. Samples were double carbon-coated under vacuum (Quorum K950 carbon coater), rotating the samples 90° between coats to ensure full coverage. Samples were viewed using a CarlZeiss GeminiSEM 300 (ACEMAC Facility, University of Aberdeen) using an accelerating voltage of 5 keV and an SE2 detector for the lowest magnification images, and 1.5 keV and an InLens secondary electron detector for all other magnifications.

Results

Corallite measurements

Sample photomicrographs showing the calyx sizes of coral genotype 1 cultured over varying seawater pCO_2 and the calyx size distributions of all corals are summarised in Fig. 2. Similar photomicrographs of all coral individuals are included in the supplementary information. The populations of calyx size within each coral are not normally distributed (Shapiro Wilk test). The *P. lutea* corals exhibit size distributions with a negative skew, i.e., most corallites had a narrow range of large calyx surface areas but there is usually a tail of smaller calices (Fig. 2b). The *P. murrayensis* corals exhibit size distributions that are more symmetrical with tails of both small and large calices. Colonial corals enlarge by budding, where parent polyps divide to produce 2 or more daughter polyps. Budding can occur outside the polyp tentacle ring (extratentacular), resulting in the daughter polyp forming on the side of the parent polyp, or can be intratentacular, resulting in the division of the parent corallite into 2 or more corallites (Veron, 1986). In the *P. lutea* skeletons we observe evidence of extratentacular budding (Fig. 1a) in all seawater pCO_2 treatments. Small corallites form on the skeletal surface adjacent to parent polyps that are similar in size to their non-budding counterparts. Extratentacular budding generates small polyps that gradually get bigger and this explains the negative skew observed in the *P. lutea* calyx size distributions. In the *P. murrayensis* skeletons budding appears to be largely intratentacular (Fig. 1c). We observe
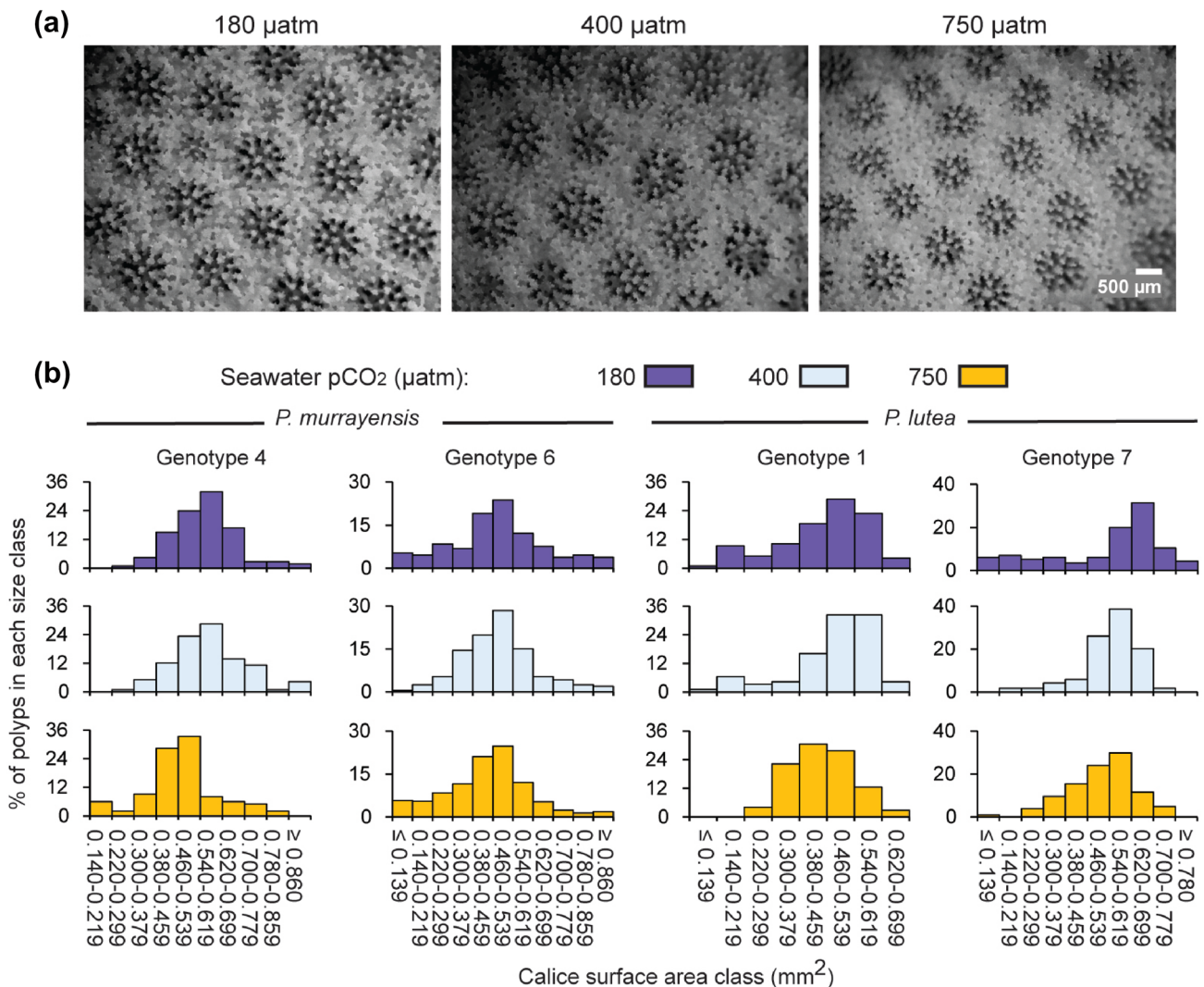

Fig. 2 **a** Photomicrographs of the skeleton surface of genotype 1 grown at contrasting seawater pCO_2 and **b** calyx size distributions in all genotypes.

relatively large corallites which contain more septae than the usual 12 and we infer that these represent polyps in the process of division. Intratentacular budding generates both large and small polyps as the dividing polyp first enlarges and then splits into 2 smaller individuals, explaining the tails of larger and smaller calices observed in the size distributions of this species. We observe intratentacular budding in all seawater pCO_2 treatments.

We compared the size distributions between seawater pCO_2 treatments within each coral genotype using the Kolmogorov–Smirnov test (Table 1). The calyx size distributions are significantly different ($p < 0.05$) between corals cultured at 750 and 400 µatm for each coral genotype but are only significantly different between 180 and 400 µatm for genotype 1. The mode (most common) calyx size class is smaller in corals cultured at 750 µatm compared to 180 µatm in 3 of the 4 genotypes (1, 4 and 7) and compared to 400 µatm in 2 of the 4 genotypes (1 and 4, Fig. 2b). The mean and median (the middle value in the data set) calyx surface areas were always smaller in corals cultured at 750 µatm compared to 400 µatm (Table 2). The Kruskal–Wallis test for equal medians indicates that medians are significantly different between corals cultured at 750 µatm compared to 400 µatm for all genotypes (Table 1).

To test for the normality of distribution in our estimates of the proportion of calyx surface area as a % of total skeletal surface we photographed and analysed additional images of the surfaces of the genotype 6 coral cultured at 400 and 750 µatm (12 and 22 images, respectively). These populations are normally distributed (Shapiro Wilk test)

and we compare the proportion of calyx surface area as a % of total skeletal surface between seawater pCO_2 treatments within each genotype using one way ANOVA. The % of the skeletal surface as calyx was significantly lower at 750 µatm compared to 400 µatm in all genotypes and significantly higher at 180 µatm compared to 400 µatm in just one genotype, G7 (Table 1, Fig. 3a).

Mean trabecula width

Porites spp. produce perforate skeletons and both the septae and coenosteum are composed of vertical trabeculae interconnected with horizontal synapticulae (Fig. 1d). These units are typically deposited at approximate right angles to each other and at approximately regular intervals resulting in an interconnecting structure with pore spaces that appear circular or oval (Fig. 4a). Sample light micrographs of trabecula and synapticulae in each coral are in the supplementary information. We measured the width of the trabecula at a distance of 1 mm from the coral surface in each coral. Trabeculae are significantly narrower in the genotype 4 and 7 corals cultured at 750 µatm compared to the corals cultured at 400 µatm (Fig. 3b, Table 1) and in the genotype 1 coral cultured at 400 µatm compared to 180 µatm. Other differences are not significant. The regular placement of trabecula and synapticulae is disturbed in genotype 7 cultured at 750 µatm and the connections between structures become more randomly organised (Fig. 4b).

Table 1 Summary of p values for statistical tests comparing calyx surface area median (Kruskal–Wallis), calyx size distribution (Kolmogorov–Smirnov), % of skeletal surface as calyx (ANOVA) and trabeculae width (ANOVA) between individuals of the same genotype cultured under different seawater pCO_2

Genotype	Calyx surface area median		Calyx size distribution		Calyx area as % of surface		Trabecula width	
	180 v 400	400 v 750	180 v 400	400 v 750	180 v 400	400 v 750	180 v 400	400 v 750
1	**0.024**	**6.6×10^{-4}**	0.081	**1.1×10^{-3}**	0.25	**0.022**	**0.019**	0.48
4	0.33	**2.3×10^{-8}**	0.15	**1.5×10^{-8}**	0.15	**1.7×10^{-3}**	1.0	**0.021**
6	0.82	**1.1×10^{-4}**	0.16	**1.3×10^{-3}**	0.29	**0.041**	1.0	0.36
7	0.19	**0.033**	**2.7×10^{-4}**	**3.1×10^{-3}**	**3.6×10^{-3}**	**7.2×10^{-5}**	0.64	**6.0×10^{-4}**

p values ≤ 0.05 are highlighted in bold

Table 2 Mean ($\pm 1\sigma$) and median calyx surface areas (mm²) in each coral genotype at each seawater pCO_2 treatment

	Mean			Median		
	180 µatm	400 µatm	750 µatm	180 µatm	400 µatm	750 µatm
Genotype 1	0.45 ± 0.13	0.48 ± 0.12	0.44 ± 0.09	0.49 (118)	0.52 (93)	0.45 (72)
Genotype 4	0.56 ± 0.14	0.58 ± 0.14	0.47 ± 0.14	0.56 (113)	0.56 (116)	0.47 (99)
Genotype 6	0.48 ± 0.19	0.45 ± 0.15	0.44 ± 0.17	0.49 (131)	0.48 (359)	0.45 (712)
Genotype 7	0.53 ± 0.20	0.55 ± 0.10	0.51 ± 0.12	0.60 (116)	0.56 (119)	0.52 (104)

n is shown in parentheses in the median side of the table
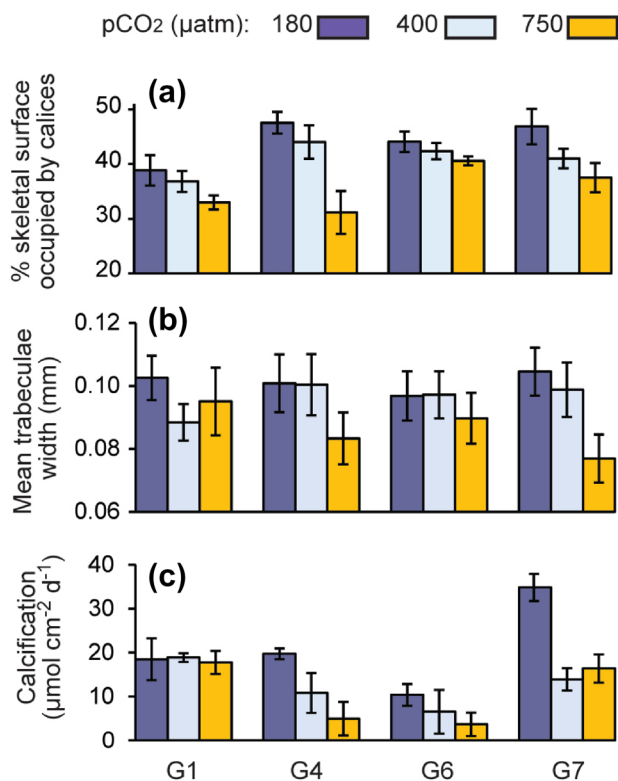
Fig. 3 Variations in **a** % of skeletal surface area occupied by calices (in contrast to coenosteum) in each coral and **b** mean trabecula width in each coral. **c** For comparison the calcification data for each coral at 25 °C is replotted from Cole et al. 2018. Error bars in each case are 95% confidence limits
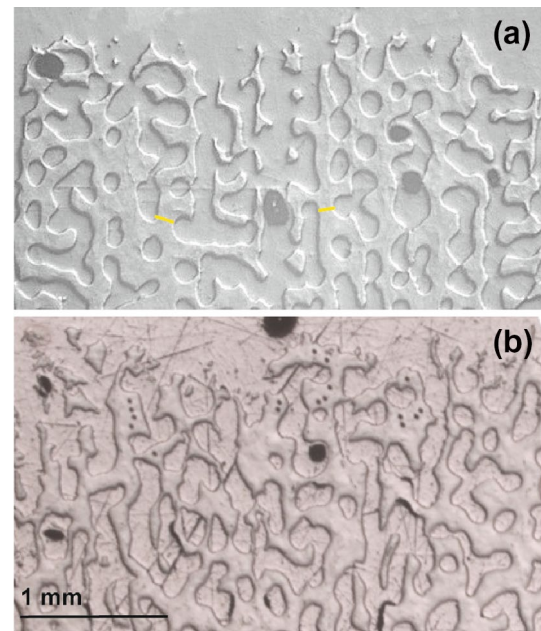

Fig. 4 Reflected light micrographs of cross sections through the outermost surface of coral genotype 7 cultured at **a** 400 µatm and **b** 750 µatm. Typical positions of trabeculae width measurements are shown by yellow lines. Ion microprobe analysis pits are visible as small black dots on the images

Scanning electron microscopy

Sample scanning electron micrographs of the corallite structure and skeletal surface are shown in Figs. 5 and 6. Additional images of each coral are included in the supplementary data. At the surface of the *Porites* spp. skeleton the extending trabeculae terminate in projections or spines which can appear as fingers radiating from a hand (Fig. 1d) and are typically 10–30 µm in height and width. The spines become noticeably more abundant at high seawater pCO_2 resulting in skeletons which appear more ornate (Figs. 5 and 6). This effect was least apparent in genotype 6 and most pronounced in genotype 7 (Fig. 6). We did not observe consistent changes in the appearance of the skeletal surface at the micron scale in response to seawater pCO_2 (Fig. 6).

Discussion

Impacts of seawater pCO_2 on skeletal morphology

Our study shows that increasing seawater pCO_2 causes significant changes in in the skeletal morphology of massive Porites spp.

corals. These changes were observed in all *Porites* spp. genotypes regardless of whether or not calcification was significantly affected by seawater pCO_2. Our study indicates that coral polyps likely become smaller in *Porites* spp. cultured at high seawater pCO_2 compared to present day values. Both the median calyx size and the proportion of skeletal surface occupied by the calices decreases significantly at 750 µatm compared to 400 µatm (Table 1). The coenosteum, connecting calices, expands to occupy a larger proportion of the coral surface at high seawater pCO_2 indicating that the coenosarc, the tissue connecting polyps, increases in area. On average, over all genotypes, mean and median calyx areas are reduced by 9 and 10%, respectively, at 750 µatm compared to 400 µatm. High seawater pCO_2 decreased corallite height in *Siderastrea siderea* by 10–15% (Horvath et al. 2016) which would have resulted in a reduction in polyp volume of the order observed in this study. Decreasing seawater pCO_2 below the modern value had little significant impact on skeletal morphology in this study. The median calyx surface was smaller, but the trabeculae were wider in the G1 corals cultured at 180 µatm compared to 400 µatm, while the proportion of skeleton occupied by calices increased in the G7 corals cultured at 180 µatm.

Our finding contrasts with other coral studies which find that calyx size increases at high seawater pCO_2 (Tambutte et al. 2015) or remains constant (Scucchia et al. 2021) and that coenosteum area decreases (Scucchia et al. 2021). The rate at which corals produce $CaCO_3$ is often reduced at high
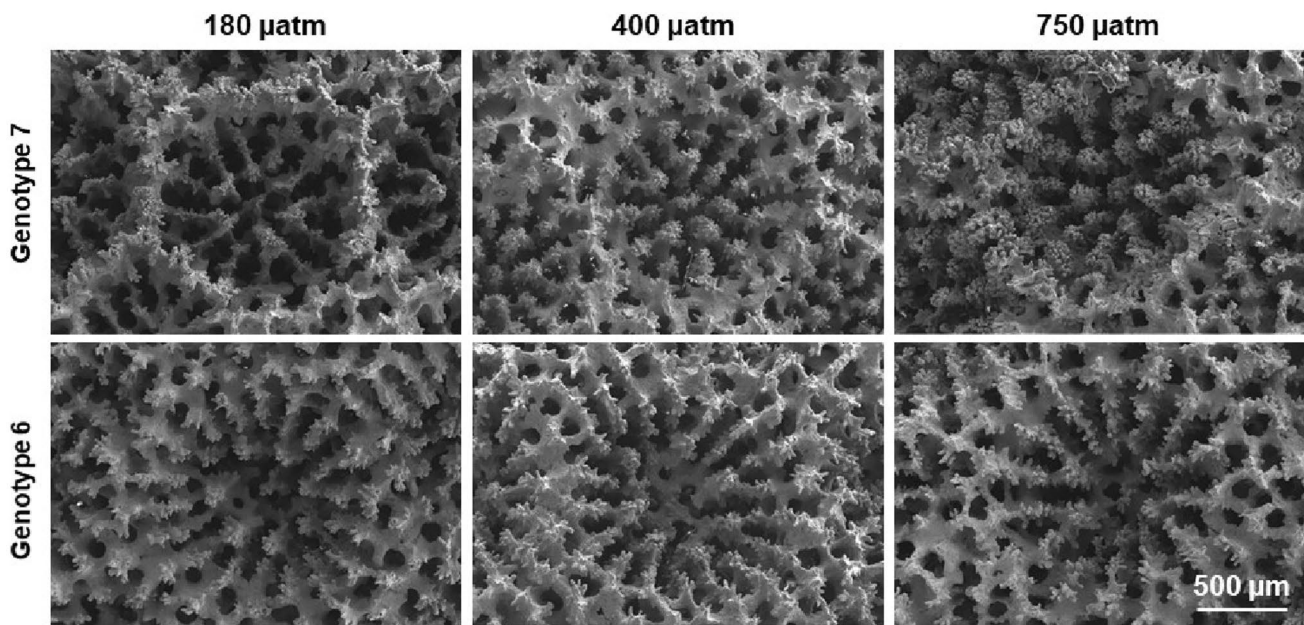
Fig. 5 Scanning electron micrographs (secondary electron images) of corallites of 2 coral genotypes cultured over a range of seawater pCO_2

seawater pCO_2 (Erez et al. 2011) and calcification rates were significantly lower in individuals of genotype 4 and 7 (but not genotypes 1 and 6) grown at 750 µatm compared to 180 µatm in the specimens examined in this study (Cole et al. 2018). Increases in calyx size are one route that corals may take to reduce the amount of $CaCO_3$ required to build the skeletons.

However, increasing calyx size requires that the polyp volume (occupying the calyx) also increases and this likely involves an energetic cost in increasing tissue biomass. We know of no other reports of reductions in polyp/calyx size in response to increasing seawater pCO_2 but heat stress is associated with a decrease in body size in polyps of Mediterranean sea anemones (Chomsky et al. 2004) and in corallites of modern solitary corals (Kersting and Linares 2019). Lasker (1981) reported a decrease in the ratio of polyp area:coenosarc area in *Montastrea cavernosa* growing at depth compared to shallow water individuals and hypothesised that this morphological adaption reduced colony maintenance costs.

Polyps in two colonial coral species (*Pocillopora damicornis* and *Oculina patagonia*) ultimately dissociated from the coenosarc under extreme pH conditions (Kvitt et al. 2015) and the reduction in polyp size suggested by our study may be a first step in this process. Although it is unclear if the reductions in calice areas observed in this study reflect a decrease in the polyp size or a reduction in $CaCO_3$ deposition, these changes in the ratio of polyp:coenosarc area likely have implications for the function of the coral. For example, the photosynthetic activities of coenosarc tissues are lower than in adjacent polyps in *Pocillopora damicornis* (Ulstrup

et al. 2006) and reducing the polyp area:coenosarc area ratio of colonies may decrease the colony primary production.

Our observation of a significant narrowing of the width of the skeletal trabecula in two of the coral genotypes (G4 and G7) at high seawater pCO_2 agrees with other studies which report a thinning of skeletal structures under ocean acidification conditions (Tambutte et al. 2015; Scucchia et al. 2021). Skeletal density but not linear extension correlates positively with seawater saturation state (Ω) in *Porites* spp. collected from multiple reefs sites spanning a range of Ω (Mollica et al. 2018) suggesting that reduced calcification in *Porites* spp. in response to high seawater pCO_2 decreases skeletal density but not linear extension. Reducing the thickness of skeletal units and increasing macro- and micro-skeletal porosity (Horvath et al. 2016; Foster et al.; 2016; Tambutte et al. 2015) all act to decrease skeletal density.

The numbers of spines formed on the skeletal growth surface of the *Porites* spp. increases at high seawater pCO_2 (Figs. 5 and 6). These spines are the first structures to develop as the coral extends its skeleton and likely form by the attachment of amorphous calcium carbonate (ACC) nanoparticles in an organic rich matrix. These transform to crystalline aragonite producing features a few microns in diameter (Drake et al. 2020). The features are termed rapid accretion deposits (RADs) and are also known as centres of calcification (Wells 1956) and early mineralisation zones (Cuif and Dauphin 2005). Aragonite fibres radiate out from the RADs to produce bundles of acicular crystals called thickening deposits (TD) which make up the bulk of the trabeculae. Coronado et al. (2019) observed a pronounced lengthening of spines at high pCO_2 in long term (> 1 year)

Fig. 6 Scanning electron micrographs of the skeleton surface of coral genotype 7 and 6 grown at contrasting seawater pCO_2. Images show the ends of trabeculae in the corallite wall (50 µm scale bar) and the skeletal surface at the micron scale (other images)
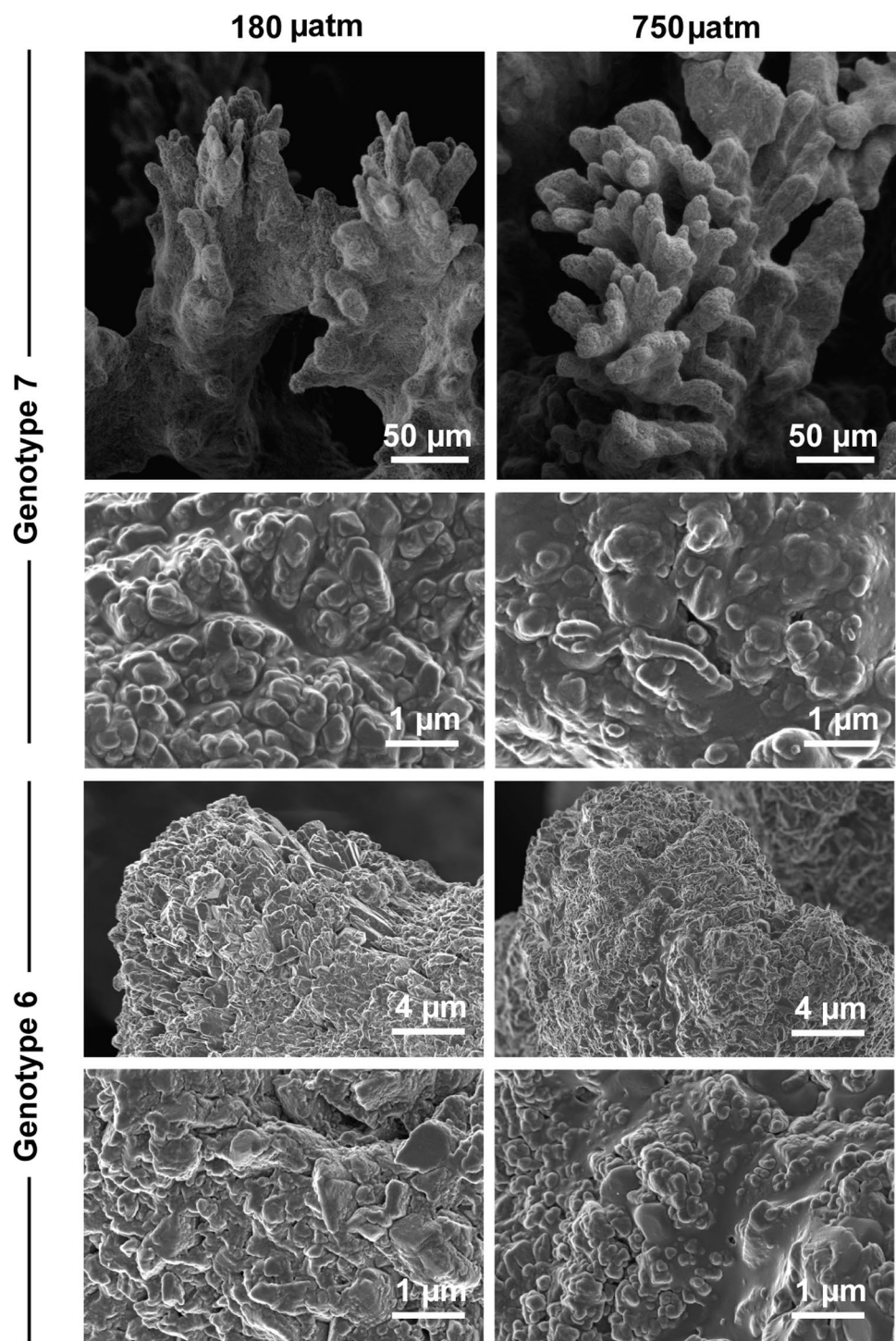
cultures of adult *Stylophorum pistillata* but Scucchia et al., (2021) reported a reduction in numbers of these features in short term (9 days) incubations of *Stylophorum pistillata* larvae. Cross sections through individual trabeculae indicate they can contain multiple RADs which formed as multiple spines on the skeletal surface, extended and became bonded together by the deposition of TDs (see Fig. 2e, Allison et al. 2001). It is unclear if the change in skeletal morphology reflects an increase in the number of spines deposited or a reduction in the production of thickening deposits that would normally obscure the spines inside the trabeculae.

Origin of changes in skeletal morphology

Increasing seawater pCO_2 can reduce the calcification rates of some corals but this does not simply manifest as

production of less skeleton of the same morphology as before but rather is accompanied by significant changes in the skeletal structure. The deposition of $CaCO_3$ must be precisely controlled to generate the highly organised and regular structures of coral skeletons (Fig. 1). This control likely occurs via enzymes and proteins which can promote and then inhibit precipitation to control $CaCO_3$ nucleation, growth and shape. Skeletons of corals cultured at high seawater pCO_2 have higher concentrations of skeletal organic material (Tambutte et al. 2015, Coronado et al. 2019) and amino acids, the building blocks of the skeletal proteins (Kellock et al. 2020). The organic matrix extracted from tropical coral skeletons affects the precipitation of $CaCO_3$ in vitro (Falini et al. 2013) and is likely to play a role in the control of skeletal formation. At high pCO_2 *Stylophora pistillata* cell cultures (Drake et al. 2018) and larvae (Scucchia et al. 2021) upregulate genes encoding for proteins of the skeletal organic matrix. This could be a mechanism to facilitate $CaCO_3$ precipitation (Drake et al. 2018) and thereby offset the reduction in seawater saturation state under ocean acidification that is likely to hamper calcification. Aspartic acid, the most abundant amino acid in the coral skeletal organic matrix (Cuif et al. 1999), inhibits aragonite precipitation at the concentrations inferred to occur at the coral calcification site (Kellock et al. 2020). The degree of inhibition is affect by the seawater saturation state suggesting that changes in the dissolved inorganic carbon chemistry of the calcification media could influence the effects of biomolecules. However, aspartic acid predominantly occurs in peptides and proteins in the skeletal organic matrix and it is unclear how these molecules influence aragonite precipitation rate and structure. RADs represent organic-rich regions of the skeleton (Von Euw et al. 2017) and increases in the concentration of the organic matrix could alter the relative proportion of RADS and TDs deposited by the coral. For example, higher skeletal organic matrix concentrations may inhibit the precipitation of TDs. Skeletal surfaces became smoother at high seawater pCO_2 in *Stylophora pistillata* (Coronado et al. 2019) and this may reflect changes in the organic matrix of the skeleton. Further work is required to elucidate the role of skeletal organic macromolecules in biomineralisation at high seawater pCO_2.

It is intriguing to consider how different coral genotypes respond to ocean acidification. Genotype G7 was the fastest calcifying coral in the study (both at high and low seawater pCO_2, Cole et al. 2018, Fig. 3c). However, at high seawater pCO_2 this genotype demonstrated the most pronounced decrease in trabeculae width, had prolific RADs and exhibited a disturbance in the regular placement of trabeculae and synapticulae, indicating that the biomineralisation process had been significantly impacted. This has parallels with culture studies which suggest that faster calcifying coral species demonstrate larger reductions in calcification in response to increased seawater pCO_2 than slow calcifying species (Comeau et al. 2014). The energetic costs of calcification, covering the extrusion of H^+ from the calcification site by Ca-ATPase (Al-Horani et al. 2003) and SOM synthesis (Allemand et al. 2011) are likely higher for faster calcifying individuals. These fast growing individuals may be unable to sustain their calcification energy budgets at high seawater pCO_2 and may be the least resilient individuals to ocean acidification.

Declarations

Conflict of interest The authors have no relevant financial or non-financial interests to disclose.

References

Al-Horani FA, Al-Moghrabi SM, de Beer D (2003) The mechanism of calcification and its relation to photosynthesis and respiration in the scleractinian coral *Galaxea fascicularis*. Mar Biol 142:419–426

Allemand D, Tambutté É, Zoccola D, Tambutté S (2011) Coral calcification, cells to reefs Coral reefs: an ecosystem in transition. Springer, pp 119–150.

Allison N, Finch AA, Sutton SR, Newville M (2001) Strontium heterogeneity and speciation in coral aragonite: implications for the strontium paleothermometer. Geochim Cosmochim Acta 65:2669–2676

Allison N, Cole C, Hintz C, Hintz K, Rae J, Finch A (2021) Resolving the interactions of ocean acidification and temperature on coral calcification media pH. Coral Reefs. https://doi.org/10.1007/s00338-021-02170-2

Barry JP, Tyrrell T, Hansson L, Plattner G-K, Gattuso J-P (2011) Atmospheric CO_2 targets for ocean acidification perturbation experiments. In: Riebesell U, Fabry VJ, Hansson L, Gattuso J-P (eds) Guide to best practices for ocean acidification research and data reporting. European Communities, Belgium

Chen PY (2015) Evaluating the economic damage of climate change on global coral reefs. Glob Environ Chang 30:12–20

Chomsky O, Kamenir Y, Hyams M, Dubinsky Z, Chadwick-Furman NE (2004) Effects of temperature on growth rate and body size in the Mediterranean Sea anemone Actinia equina. J Exp Mar Biol Ecol 313:63–73

Cole C, Finch A, Hintz C, Hintz K, Allison N (2016) Understanding cold bias: variable response of skeletal Sr/Ca to seawater pCO_2 in acclimated massive *Porites* corals. Scientific Reports 6.

Cole C, Finch A, Hintz C, Hintz K, Allison N (2018) Effects of seawater pCO_2 and temperature on calcification and productivity in the coral genus *Porites* spp.: an exploration of potential interaction mechanisms. Coral Reefs 37:471–481

Comeau S, Edmunds PJ, Spindel NB, Carpenter RC (2014) Fast coral reef calcifiers are more sensitive to ocean acidification in short-term laboratory incubations. Limnol Oceanogr 59:1081–1091

Coronado I, Fine M, Bosellini FR (2019) Impact of ocean acidification on crystallographic vital effect of the coral skeleton. Nat Commun 10:2896. https://doi.org/10.1038/s41467-019-10833-6

Crook ED, Potts D, Rebolledo-Vieyra M, Hernandez L, Paytan A (2012) Calcifying coral abundance near low-pH springs: implications for future ocean acidification. Coral Reefs 31:239–245

Cuif JP, Dauphin Y (2005) The two-step mode of growth in scleractinian coral skeletons from the micrometre to the overall scale. J Struct Biol 150:319–333

Cuif JP, Dauphin Y, Gautret P (1999) Compositional diversity of soluble mineralizing matrices in some recent coral skeletons compared to fine-scale growth structures of fibres: discussion of consequences for biomineralization and diagenesis. Int J Earth Sci 88:582–592

Drake JL, Schaller MF, Mass T, Godfrey L, Fu A, Sherrell RM, Rosenthal Y, Falkowski PG (2018) Molecular and geochemical perspectives on the influence of CO_2 on calcification in coral cell cultures. Limnol Oceanogr 63:107–121

Drake JL, Mass T, Stolarski J, Von Euw S, van de Schootbrugge B, Falkowski PG (2020) How corals made rocks through the ages. Glob Change Biol 26:31–53

Edmunds PJ (2012) Effect of pCO_2 on the growth, respiration, and photophysiology of massive *Porites* spp. in Moorea French. Poly Marine Biol 159:2149–2160

Elhadj S, De Yoreo JJ, Hoyer JR, Dove PM (2006) Role of molecular charge and hydrophilicity in regulating the kinetics of crystal growth. Proc Natl Acad Sci USA 103:19237–19242

Erez J, Reynaud S, Silverman J, Schneider K, Allemand D (2011) Coral calcification under ocean acidification and global change. In coral reefs: an ecosystem in transition. Springer.

Fabricius KE, Langdon C, Uthicke S, Humphrey C, Noonan S, De'ath G, Okazaki R, Muehllehner N, Glas MS, Lough JM (2011) Losers and winners in coral reefs acclimatized to elevated carbon dioxide concentrations. Nat Clim Chang 1:165–169

Falini G et al (2013) Control of aragonite deposition in colonial corals by intra-skeletal macromolecules. J Struct Biol 183:226–238

Falini G, Fermani S, Goffredo S (2015) Coral biomineralization: a focus on intra-skeletal organic matrix and calcification. Semin Cell Dev Biol 46:17–26

Foster T, Falter JL, McCulloch MT, Clode PL (2016) Ocean acidification causes structural deformities in juvenile coral skeletons. Sci Adv 2(2):e1501130

Herman A, Addadi L, Weiner S (1988) Interactions of sea-urchin skeleton macromolecules with growing calcite crystals—a study of intracrystalline proteins. Nature 331:546–548. https://doi.org/10.1038/331546a0

Horvath KM, Castillo KD, Armstrong P, Westfield IT, Courtney T, Ries JB (2016) Next-century ocean acidification and warming both reduce calcification rate, but only acidification alters skeletal morphology of reef-building coral *Siderastrea siderea*. Sci Rep 6:1–12

Kellock C, Cole C, Penkman K, Evans D, Kroger R, Hintz C, Hintz K, Finch A, Allison N (2020) The role of aspartic acid in reducing coral calcification under ocean acidification conditions. Sci Rep. https://doi.org/10.1038/s41598-020-69556-0

Kersting DK, Linares Prats C (2019) Living evidence of a fossil survival strategy raises hope for warming-impacted corals. Sci Adv 5(10):eaax2950

Kim YY, Carloni JD, Demarchi B, Sparks D, Reid DG, Kunitake ME, Tang CC, Duer MJ, Freeman CL, Pokroy B, Penkman K (2016) Tuning hardness in calcite by incorporation of amino acids. Nat Mater 15:903–910

Kvitt H, Kramarsky-Winter E, Maor-Landaw K, Zandbank K, Kushmaro A, Rosenfeld H, Fine M, Tchernov D (2015) Breakdown of coral colonial form under reduced pH conditions is initiated in polyps and mediated through apoptosis. Proc Natl Acad Sci 17:2082–2086

Lasker HR (1981) Phenotypic variation in the coral *Montastrea cavernosa* and its effects on colony energetics. Biol Bull 160:292–302

Mollica NR, Guo W, Cohen AL, Huang K-F, Foster GL, Donald HK, Solow AR (2018) Ocean acidification affects coral growth by reducing density, Proc. Nat. Acad. Sci., 115 (8) 1754–1759; DOI: https://doi.org/10.1073/pnas.1712806115.

Scucchia F, Malik A, Zaslansky P, Putnam HM, Mass T (2021) Combined responses of primary coral polyps and their algal endosymbionts to decreasing seawater pH. Proc R Soc B 288:20210328

Tambutté E, Venn AA, Holcomb M, Segonds N, Techer N, Zoccola D, Allemand D, Tambutté S (2015) Morphological plasticity of the coral skeleton under CO_2-driven seawater acidification. Nat Commun 6:1–9

Ulstrup KE, Ralph PJ, Larkum AW, Kühl M (2006) Intra-colonial variability in light acclimation of zooxanthellae in coral tissues of *Pocillopora damicornis*. Mar Biol 149:1325–1335

Venn AA, Tambutte E, Holcomb M, Allemand D, Tambutte S (2011) Live tissue imaging shows reef corals elevate pH under their calcifying tissue relative to seawater. PLoS One 6:e20013

Venn AA, Tambutte E, Holcomb M, Tambutte S (2013) Impact of seawater acidification on pH at the tissue-skeleton interface and calcification in reef corals. Proc Natl Acad Sci 110:1634–1639

Von Euw S, Zhang Q, Manichev V, Murali N, Gross J, Feldman LC, Gustafsson T, Flach C, Mendelsohn R, Falkowski PG (2017) Biological control of aragonite formation in stony corals. Science 356:933–938

Wells JW (1956) Scleractinia. In: Moore RC (ed) Treatise on Invertebrate paleontology, part F, coelenterata. Univ. of Kansas Press, Lawrence, pp 328–444